N92-27791

Application of Ceramic Superconductors in High Speed Turbines

C. K. McMichael[a], M. A. Lamb[b], M. W. Lin[c], K. B. Ma and W. K. Chu
The Texas Center for Superconductivity at the University of Houston

(a) C. K. McMichael is an undergraduate fellow from the University of Houston.
(b) M. A. Lamb is an undergraduate fellow from the University of Houston.
(c) M. W. Lin is an undergraduate fellow from the California Institute of Technology.

SUMMARY

A turbine system was modified to adapt melt-textured $Y_1Ba_2Cu_3O_{7-\delta}$ (YBCO) with high energy permanent magnets to form a hybrid superconducting magnetic bearing (HSMB). The HSMB/turbine prototype has achieved a static axial thrust capacity exceeding 41 N/cm^2 (60 psi) and a radial magnetic stiffness of 7 N/mm in a field cooled state at 77 K. A comparison was made between different configurations of magnets and superconductor for radial stability, axial instability, and force hystereses. This systematic study led to a greater understanding of the interactions between YBCO and high energy permanent magnets to define design parameters for high rotational devices ultilizing the HSMB design.

INTRODUCTION

The advent of high temperature superconductors (HTS) which exhibit type II behavior (pinning effect [1]) has created many possible applications for bulk materials such as $Y_1Ba_2Cu_3O_{7-\delta}$ (YBCO). The ability to levitate passively machinery which rotates at high speeds without active control systems or complex pneumatics with almost zero energy consumption warrants investigation. As low energy consumption is a crucial consideration for operation in a cryogenic environment, it would seem that this requirement makes high temperature superconductors (HTS) ideal for such applications. A simple superconducting magnetic bearing (SMB) utilizing the pinning effect has been demonstrated by the ubiquitous observation of a pair of HTS stators field cooled around a set of permanent magnets [2]. With the onset of higher Jc materials produced by texturing processes [3, 4], and with further increases being very promising with neutron and high energy proton irradiation [5, 6] of bulk YBCO, the corresponding increase in flux pinning could enable oriented samples of YBCO to trap magnetic flux on the same order of magnitude as that of rare earth permanent magnets [7, 8]. Using such high flux trapping samples would raise the levitation and magnetic stiffness effectively. Still, there is a problem with the SMBs in terms of gap stabilization over long periods of time [9].

It is now becoming feasible to use bulk superconductors in the design of high speed rotational devices requiring multi-axis passive bearing traits. In this paper, we present the hybrid superconducting magnetic bearing (HSMB)/turbine prototype (Fig. 1) which exhibits multi-axis stability in a passive levitated state.

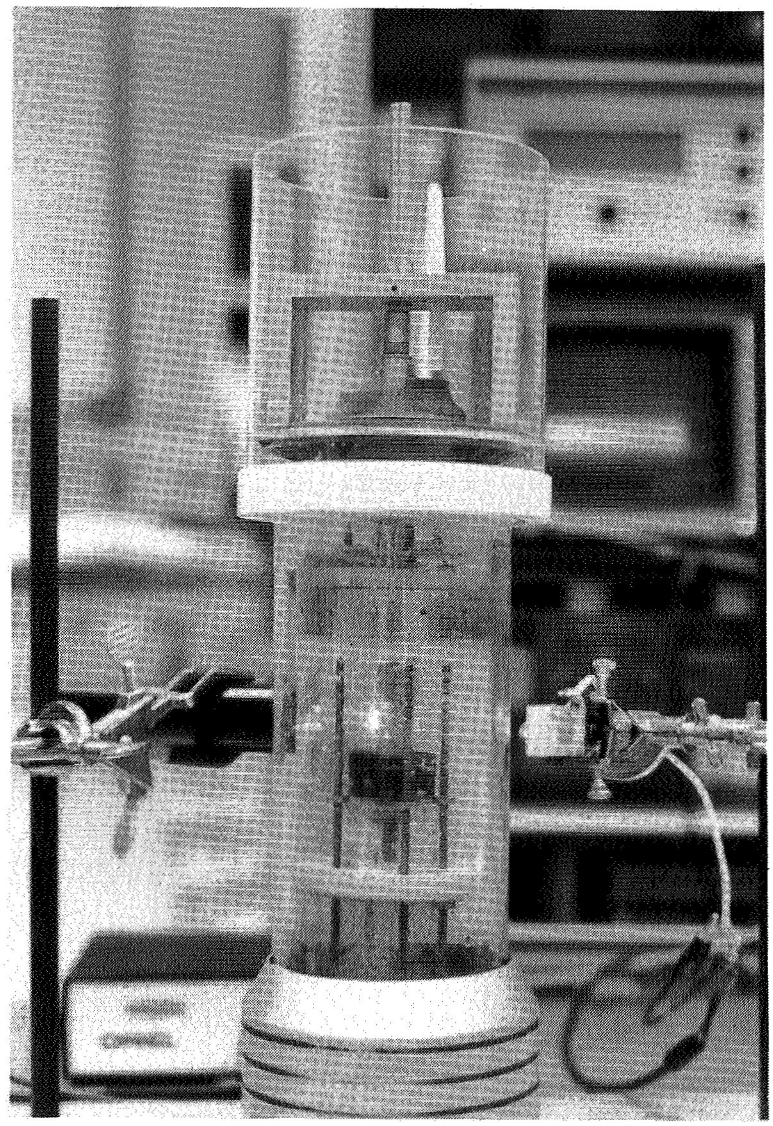

Fig. 1 Photograph of our prototype HSMB.

EXPERIMENTAL

This HSMB/turbine (Fig. 2) is constructed with melt-textured YBCO as the stators and NbFeB as the rotor permanent magnets with a surface field at the center of a pole face of 0.429 T. In the test model, two melt-textured tubes (1.8 cm length, 1.2 cm ID, 2.5 cm OD) were sealed to a 5.7 cm long glass tube to form a journal bearing set. The thrust HTS bearing member was a melt-textured disk (2 cm diameter, 4.75 mm thick) which was sealed to the end of the journal bearing set. The journal and thrust permanent magnet bearing members were aligned to maximize the magnetic field repulsion strength. The rotor shaft (1 cm diameter, 10 cm long) contained three simple dipoles, one at the top for an attractive thrust, one for the journal, and one for repulsive thrust at the bottom. The entire HSMB assembly was immersed in a glass dewar containing liquid nitrogen, while a high pressure gas nozzle was used to drive the turbine.

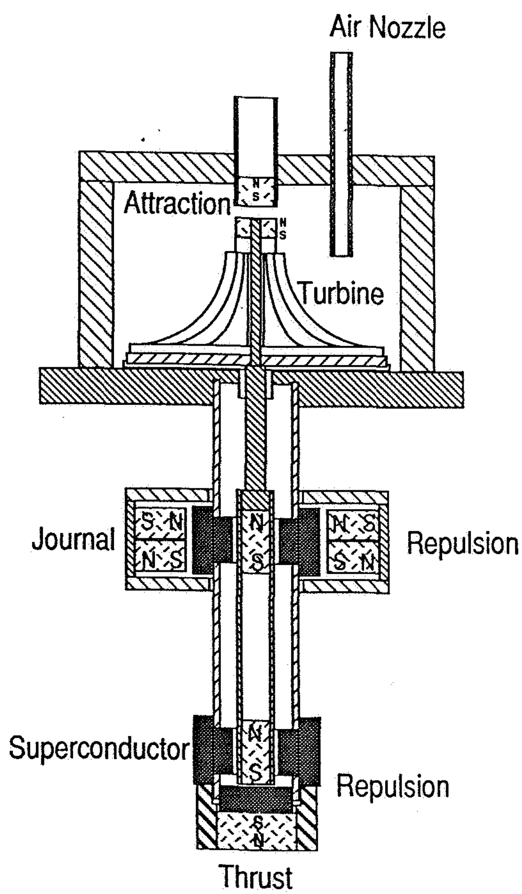

Fig. 2 Drawing of our prototype HSMB.

In a static setup, force measurements were conducted on each bearing element using a cantilever beam-strain gauge apparatus [10]. A stationary cold stage which held the superconductor and magnet assemblies were attached to an optical table. The forces acting within two of the three bearing components were assembled individually and measured. Magnet-magnet attraction and repulsion forces were measured as a function of displacement from the central axis for various gap distances (Fig. 3, 4).

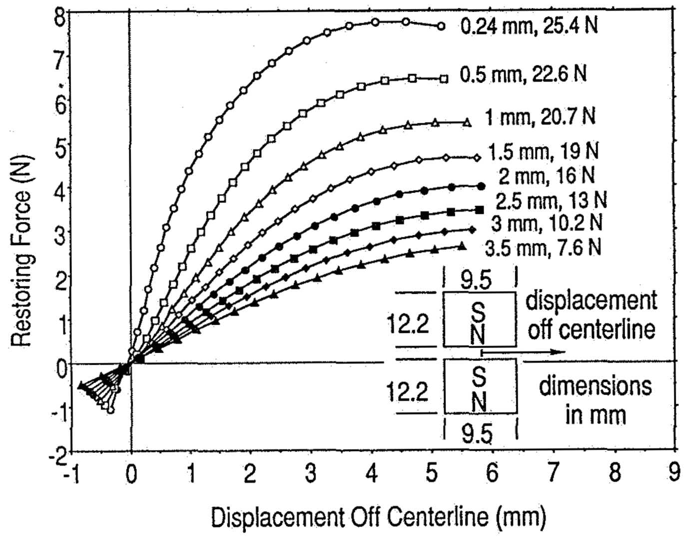

Fig. 3 Radial component of restoring force as a function of radial displacement off central axis for the top bearing component.

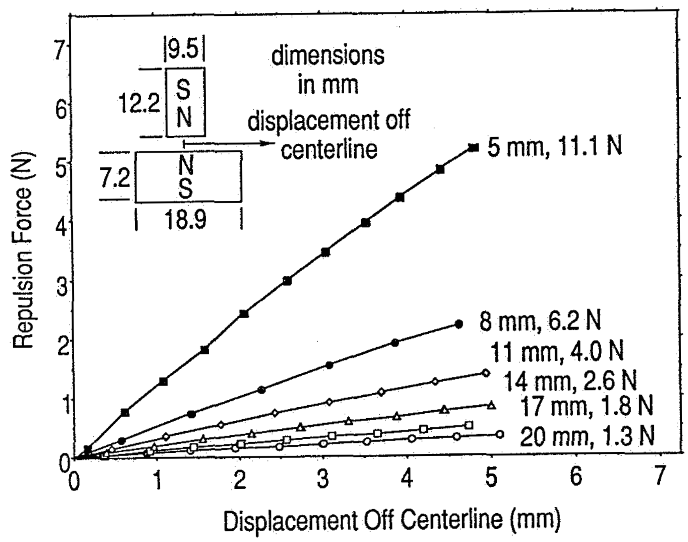

Fig. 4 Radial component of repulsion force as a function of radial displacement off central axis for the bottom bearing component.

Radial and axial hystereses were measured to compare HSMB, field cooled superconductor, and magnet-magnet thrust configurations (Fig. 5, 6).

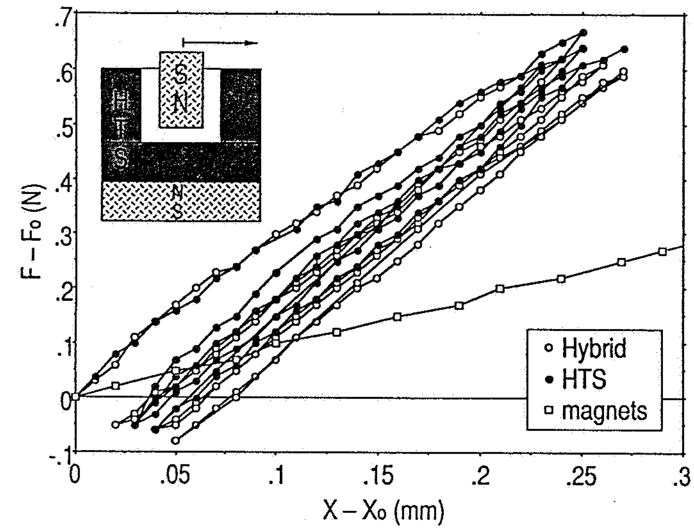

Fig. 5 Radial hysteresis loops - change of force from the initial setup value (different for the three separate cases) as the magnet is displaced across the HTS well, as a function of the displacement from the initial point near the center.

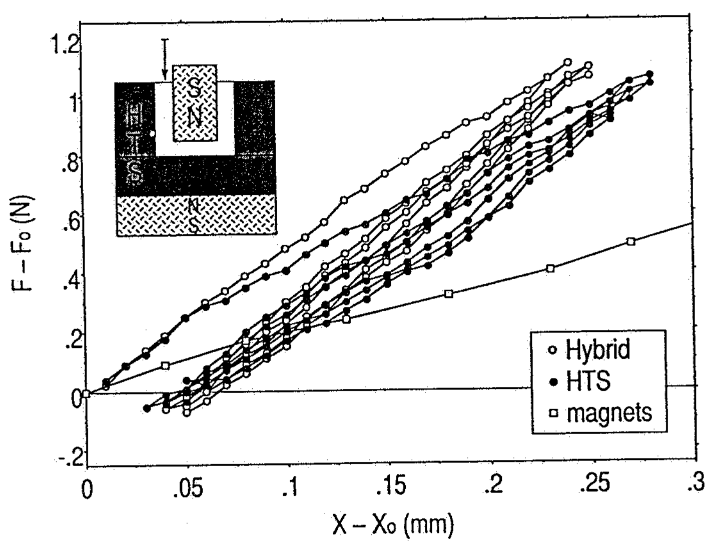

Fig. 6 Axial hysteresis loops - change of force from the initial setup value (different for the three separate cases) as the magnet is lowered into the HTS well, as a function of the displacement from the initial point.

Journal configurations were treated similarly (Figs. 7, 8, 9).

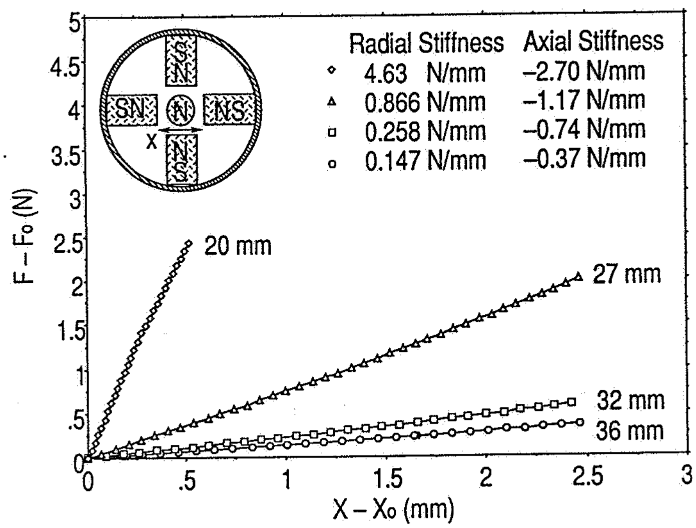

Fig. 7 Restoring forces for the central magnet in the central configuration - change of force from the initial setup value as the central magnet is moved in the plane of the set of four outer magnet pairs, along a line joining two opposite magnet pairs, as a function of the displacement from the initial point near the center.

RESULTS AND DISCUSSION

From the data in Figs. 5 and 6, there is apparently no significant difference between the hybrid and the FC HTS by itself in so far as the stiffness of the configuration is concerned. Even in the axial direction, the effect of the stator magnet is not quite discernible until displacements larger than 0.2 mm. are reached. The net effect of the stator magnet seems to be boosting up the thrust only. Certainly, we do not have to be concerned with the stability provided by the FC HTS being compromised by the presence of an additional magnet in this configuration. It remains to be seen as to how much additional thrust we can get out of the magnet by decreasing the thickness of the intervening HTS layer without compromising excessively on the stability. It is also interesting to ask whether that intervening HTS layer can be eliminated altogether. We believe that there are no inherent principles preventing this from happening.

In contrast, a careful examination of the data in Figs. 8 and 9 shows that the effects from the stator magnet are conspicuous in the journal configurations.

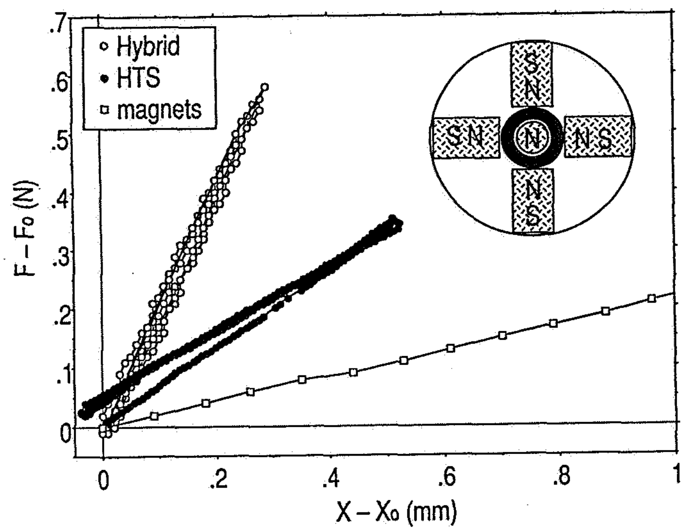

Fig. 8 Radial hysteresis loops - change of force from the initial setup value (different for the three separate cases) as the magnet is displaced across the HTS doughnut, as a function of the displacement from the initial point near the center.

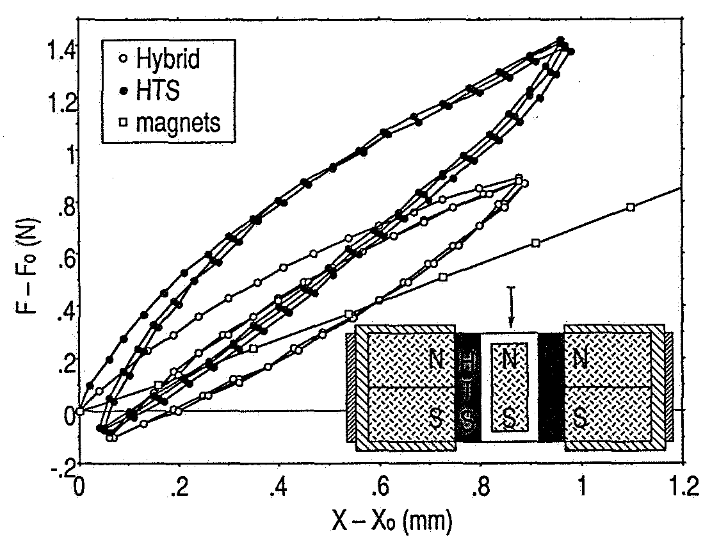

Fig. 9 Axial hysteresis loops - change of force from the initial setup value (different for the three separate cases) as the magnet is poked through the HTS doughnut, as a function of the displacement from the initial point.

The stator magnets are not intended to create an extra thrust, here. They are added to exchange some axial stability for radial stability. Qualitatively, we can see that the radial stiffness of the hybrid is enhanced, while the axial stiffness is suppressed from the FC HTS case, just as the corresponding stiffnesses of the stator magnet configuration would lead us to expect. Also noteworthy are the differences in the characteristics of the hysteresis loops. The axial hysteresis loops are much wider than the radial hysteresis loops for the journal configurations. There is almost no tendency for the loop to drift in the direction of the initial displacement, whereas this was quite pronounced on the thrust configuration. We believe that the former effect is a consequence of the relative geometries of the magnetic field, the superconductor surface and the direction of the displacement, while the latter is a manifestation of force creep.

Overall, this prototype bearing that we have constructed can support a thrust of 41 N/cm^2 or 60 psi, normalized to the cross-section of the shaft. Of these, about one third comes from the repulsion between the two magnets in the thrust bearing at the bottom, while the remaining two thirds comes from the attraction between two magnets at the top. The bottom thrust bearing has a net radial instability, while the top thrust bearing has a net axial instabilty. Since these two instabilities stem from forces acting on different ends of the shaft, they would combine to produce a tilt instability even if they appear to cancel each other out. This is just another instance illustrating Earnshaw's theorem [11]. With the HTS pieces, the journal bearing in the middle functions to stabilize against the axial instability of the top bearing, while the HTS well of the thrust bearing at the bottom functions to stabilize against the radial instability from the repelling magnets located in its vicinity. Further refinement of the balance between axial and radial instabilities can be made by adjusting the stator magnets in the journal bearing. When assembled, the overall stiffness of the bearing would be several N/mm, variously distributed amongst the three bearing components.

Finally, we want to add that all our force measurements were performed on a time scale of a fraction of a second. Therefore, we can expect our stiffnesses to apply to vibrational phenonema of a few Hz. Other works [12] have indicated that the stiffnesses are relatively independent of frequency. Thus, our results may still be valid over a wider range of frequencies. This awaits further investigation.

REFERENCES

1. M. Murakami, T. Oyama, H. Fujimoto, T. Tagughi, S. Gotoh, Y. Shiohara, N. Koshizuka and S. Tanaka, Jap. J. Appl. Phys. 26, L1991 (1990).
2. C. K. McMichael, K. B. Ma, M. W. Lin, M. A. Lamb, R. L. Meng, Y. Y. Xue, P. H. Hor and W. K. Chu, to be published in Appl. Phys. Lett.
3. R. L. Meng, C. Kinalidis, Y. Y. Sun, L. Gao, Y. K. Tao, P. H. Hor and C. W. Chu, Nature 345, 326 (1990).
4. S. Tanaka, IEEE Trans. MAG (1991).
5. P. H. Hor, Z. J. Huang, L. Gao, R. L. Meng, Y. Y. Xue Y. C. Jean , J. Farmer and C. W. Chu, Mod. Phys. Lett. B 703, 4 (1990).
6. L. Civale, A. D. Marwick, M. W. McElfresh, T. K. Worthington, A. P. Malozemoff, and F. H. Holzberg, J. R. Thompson, M. A. Kirk, Phys. Rev. Lett., 65, 1164 (1990).
7. A. D. Crapo and J. D. Loyd, IEEE Tran. Mag., 27 2244 (1990).
8. R. Weinstein, et al., Appl. Phys. Lett. 56, 1475 (1991).
9. F. C. Moon and J. R. Hull, 25th IECEC 3, 425 (1990).
10. F. C. Moon, M. M. Yanoviak, and R. Ware, Appl. Phys. Lett. 52, 1534 (1988).
11. S. Earnshaw, "On the Nature of the Molecular Forces which Regulate the Constitution of the Luminferous Ether," Trans. Camb. Phil. Soc. 7, pp. 97-112, (1842).
12. S. A. Basinger, J. R. Hull, and T. M. Mulcahy, Appl. Phys. Lett. 57, 2942 (1990).